Mathematical Modelling, Sensitivity Analysis and Optimal Control in Cyclone Intensity: Exploring Stability and Strategies

¹Debasri Samanta; ² Rajib Kumar Dolai; ³ Manotosh Mandal

- ¹ Research Scholar, Department of Physics, Vidyasagar University, Midnapore, West Bengal, India
- ² Assistant Professor, Department of Economics, Tamralipta Mahavidyalaya, Tamluk, West Bengal, India
- ³ Assistant Professor, Department of Mathematics, Tamralipta Mahavidyalaya, Tamluk, West Bengal, India

Corresponding Author: Debasri Samanta

Abstract: This study develops a mathematical model to examine the dynamics of cyclone intensity under climate change and proposes an optimal control strategy to mitigate its impacts. Recent observations indicate a marked rise in tropical cyclone intensity over past decades, largely driven by increasing global temperatures. The model captures the interactions between sea surface temperature, accumulated cyclone energy, and cyclone intensity. By applying Pontryagin's Maximum Principle, we derive optimal control trajectories aimed at minimizing cyclone intensity while maintaining system stability. Numerical simulations reveal that adaptive temperature reduction strategies significantly outperform fixed controls, leading to lower cyclone intensity and enhanced system resilience over time. The analysis further establishes that the system's equilibrium points are both locally and globally asymptotically stable, ensuring the feasibility of long-term solutions. Sensitivity analysis highlights the temperature growth rate and control effort as the most influential parameters, high lighting the importance of targeted interventions.

Keywords: Environmental Management, Pontryagin's Maximum Principle, Climate mitigation, Numerical simulations, Optimal Control

1. Introduction

Tropical cyclones are among the most devastating natural disasters, causing immense destruction to human lives, infrastructure, and ecosystems. Their increasing frequency and intensity in recent decades have been strongly linked to rising global temperatures, a consequence of anthropogenic climate change. Warmer sea surface temperatures (SSTs) act as a primary energy source for cyclone formation, fuelling stronger winds, extending storm lifespans, and significantly amplifying their destructive potential. This intensification is particularly pronounced in tropical and subtropical regions, where elevated SSTs have led to an increase in high-intensity cyclones, resulting in devastating storm surges, torrential rainfall, and large-scale flooding. However, cyclones are not merely passive consequences of climate change; they actively influence the climate system by redistributing ocean heat, altering atmospheric circulation patterns, and driving oceanic mixing. This complex interplay between cyclone activity and climate variability makes long-term cyclone forecasting particularly challenging, necessitating the development of advanced models that account for both climate change and cyclone-induced feedback mechanisms. Mathematical modelling has emerged as a crucial tool for analysing the nonlinear dynamics of tropical cyclones. Traditional models, rooted in thermodynamics and fluid dynamics, have significantly improved storm forecasting by simulating formation, intensification, and dissipation processes. However, many of these models overlook the long-term influence of climate change and the potential role of human intervention in mitigating cyclone intensity.

Climate change is significantly influencing tropical cyclones (TCs), as explored through various modelling, observational, and theoretical approaches. For instance, Walsh et al. (2000) found that storm intensities increased under enhanced greenhouse conditions, although their significance was constrained by vertical wind shear and model resolution. Similarly, Tsuboki et al. (2015) projected that future super typhoons could reach extreme intensities in a warming climate. In the same vein, Wu et al. (2022) and van (2024) further reinforced theoretical evidence of intensification; however, they also highlighted uncertainties stemming from data limitations, natural variability, and model biases, which complicate basin-wide assessments. In addition to storm physics, the socioeconomic and ecological dimensions of TC impacts have been emphasized. For example, Mendelsohn et al. (2012) demonstrated that economic losses from stronger storms could more than double, whereas Kropf et al. (2025) and Hülsen et al. (2025) projected long-term vulnerability of terrestrial ecosystems. The devastating human consequences of extreme storms were further illustrated by Knabb et al. (2005), who documented Hurricane Katrina as one of the most destructive hurricanes in U.S. history, reaching Category 5 intensity. At a regional scale, Gupta et al. (2019) reported severe impacts in the Bay of Bengal, while Li et al. (2025) showed that rapid intensification events in the Arabian Sea have doubled since 2013 due to rising SSTs. Supporting these observations, Hill et al. (2010) and Bhatia et al. (2018) predicted that future TCs will likely become more frequent and intense, exhibiting larger pressure deficits and increased precipitation rates. Advances in modelling and data-driven approaches have also provided valuable insights. For instance, Chen et al. (2025) reconstructed cyclone wind profiles to reveal increases in extreme storms, Wu et al. (2025) linked SST rises to intensification, and Varalakshmi et al. (2023) improved forecasts in India using hybrid deep learning techniques. Moreover, Sun et al. (2022) identified a threshold SST governing cyclone strengthening, whereas Régibeau-Rockett et al. (2024) demonstrated that mechanical efficiency declines at very high SSTs due to atmospheric moisture effects—thus underscoring the complex role of ocean temperatures. Several classic contributions have also shaped the theoretical foundation of TC research. Chan et al. (2001) identified an SST threshold of approximately 27°C for TC development, while Emanuel (2005) introduced the power dissipation index (PDI) to measure hurricane destructiveness, showing a marked increase since the 1970s as storms became stronger and longer-lived. In addition, Dare et al. (2011) reported that SSTs cool by an average of -0.9°C after TC passage, with recovery times varying by storm intensity and seasonality. Likewise, Chavas et al. (2017) established a theoretical relationship between central pressure deficit and peak wind speed, thereby improving the understanding of TC intensity. Similarly, Holland (1997) described the acceleration of maximum potential intensity (MPI) above 26°C. Looking ahead, Knutson et al. (2010, 2020) projected that although the overall frequency of TCs may decrease by 6-34%, their intensity is expected to increase by 2-11%. Furthermore, Hart et al. (2001) found that 46% of Atlantic TCs transitioned to extratropical storms, primarily affecting the northeastern United States, Canada, and Europe. Finally, Vecchi et al. (2007) concluded that regional warming patterns, rather than localized SST increases alone, play a more decisive role in shaping TC potential intensity.

Collectively, these studies highlight the central role of SST in shaping cyclone strength and frequency; however, they largely focus on natural warming trajectories rather than policy-driven cooling or stabilization of SSTs. This points to a crucial gap: while the intensifying effect of rising SSTs on TCs is well established, limited attention has been given to how climate mitigation policies that regulate SST might alter cyclone behavior. To address this gap, the present study develops a dynamical model that incorporates a control parameter representing policy strategies, thereby providing a novel framework to assess how temperature regulation could influence cyclone risks in a changing climate.

2. Model formulation

Cyclone intensity is driven by the interaction of accumulated cyclone energy, sea surface temperature, and external controls. Warm ocean waters enhance storm intensity through latent heat, while environmental factors like wind shear, land interaction, and ocean cooling limit growth. Accumulated cyclone energy reflects the storm's energy, influenced by ocean temperature and atmospheric conditions. Sea surface temperature evolves due to natural warming, cyclone-induced mixing, and climate mitigation efforts. Global interventions, such as greenhouse gas reduction and ocean cooling, regulate sea surface temperature and help control cyclone intensity.

We assume that at time t, S(t), E(t), and T(t) represent the level of cyclone intensity, accumulated cyclone energy, and the sea surface temperature respectively.

The level of cyclone intensity is driven by the interplay between sea surface temperature and accumulated cyclone energy. Warmer sea surface temperatures supply the latent heat necessary to sustain cyclones, while accumulated cyclone energy enhances storm intensity; however, excessive warming induces saturation effects, increasing wind shear and dry air intrusion, which limit further intensification. We assume that α is the energy transfer coefficient that represents the cyclone energydriven intensification process. Physically, it suggests that the rate of change of cyclone intensity increases proportionally to both the current strength of the cyclone and the amount of energy stored in the system. This reflects a positive feedback mechanism: as the cyclone becomes more intense and the surrounding environment holds more energy, the cyclone can strengthen even further.

Similarly, we introduce β as the sensitivity coefficient, which governs the temperaturedependent growth of cyclone intensity, modulated by a saturation effect. At lower sea surface temperature (SST) levels, even small increases in temperature can significantly enhance cyclone strength because additional thermal energy becomes available to fuel storm development. However, as SST continues to rise, various environmental constraints — such as increased atmospheric stability, enhanced upper-ocean heat mixing, and limitations in moisture supply or outflow ventilation — begin to cap the cyclone's potential intensity. This leads to a phenomenon known as saturation, where further increases in SST contribute progressively less to cyclone growth, thereby preventing unbounded intensification. To capture the natural constraints on warminginduced intensification, we assume that σ is the energy transfer rate associated with SST dynamics, and m represents a temperature threshold beyond which the ocean can no longer sustain unchecked warming. The term follows a logistic-type behavior: when the SST T is relatively small compared to m, the factor $\left(1 - \frac{T}{m}\right)$ remains close to 1, allowing SST to increase almost linearly. However, as T becomes larger and approaches the value of m, the factor steadily decreases toward zero, slowing the SST growth and reflecting the system's natural resistance to excessive heating. Finally, cyclone dissipation, influenced by processes such as landfall, ocean surface cooling, and atmospheric instability, is modelled by the linear decay term µS, where µ represents the dissipation rate. This term accounts for the natural weakening of cyclones over time due to environmental and surface interactions that oppose intensification.

The evolution of accumulated cyclone energy (ACE) is primarily influenced by the interactions between sea surface temperature (SST) and cyclone intensity. Warmer SSTs provide the essential latent heat that fuels cyclone activity, while stronger cyclones extract more energy from the environment, thereby increasing the accumulated cyclone energy. However, excessive warming can introduce inhibiting factors, such as enhanced vertical wind shear and dry air intrusion, which disrupt storm organization and limit further energy accumulation. We assume that ρ is the energy extraction coefficient, representing the efficiency with which cyclones draw available oceanic heat into kinetic energy. Physically, this coefficient implies that

higher sea surface temperatures and existing levels of cyclone energy together promote the growth of accumulated cyclone energy, reflecting a positive feedback loop where favourable oceanic conditions intensify storm development.

To account for the regulation of ACE through cyclone intensity, we introduce τ as the intensity-energy coupling coefficient. This coefficient captures the idea that while stronger cyclones can tap into more energy, they also trigger internal structural changes and increased interaction with environmental conditions that moderate further energy accumulation. Thus, τ acts as a balancing factor that prevents unlimited growth of accumulated energy as cyclone strength rises. Additionally, we incorporate y as the natural dissipation rate of accumulated cyclone energy, representing the combined effects of surface frictional losses and turbulent mixing with the surrounding atmosphere. This coefficient ensures that without continuous energy input from warm ocean surfaces, accumulated cyclone energy gradually decays over time due to environmental and surface processes.

The evolution of sea surface temperature (SST) is a critical driver of cyclone dynamics and energy accumulation. SST increases are primarily influenced by external heat fluxes, ocean-atmosphere interactions, and internal oceanic processes. Warmer SSTs enhance the available latent heat for cyclones, but feedbacks from cyclonic activity and vertical mixing processes can limit or even reduce SST over time. We assume ϕ as the rate of temperature increase due to climate change, capturing the baseline rise in sea surface temperature (SST) driven by external factors, such as solar radiation and atmospheric heat fluxes. Cyclone-induced cooling is modelled by ξ , where ξ quantifies the efficiency of energy-driven ocean mixing in reducing SST. As cyclones interact with the ocean, they enhance vertical mixing, drawing cooler waters from below the surface and lowering the local SST. The strength of this cooling effect is proportional to both the cyclone energy E and the SST T, with ξ determining the efficiency of this process.

In addition, we introduce u as the global temperature reduction effort coefficient, representing the impact of human interventions such as climate change mitigation policies, carbon emission reductions, and strategies aimed at curbing SST increases. These efforts act as an additional cooling influence on SST dynamics. However, the effectiveness of such measures diminishes as SST becomes very high, reflecting practical limitations in how much global action can offset the thermal inertia of the ocean. Finally, n is introduced as a saturation threshold parameter that modulates the efficiency of background cooling efforts. When SST levels are relatively low, the global temperature reduction measures are more effective; but as SST rises closer to n, the impact of cooling interventions weakens, realistically capturing the challenges of reversing warming trends in a heavily heated ocean system.

By using the above assumption we formulate the mathematical model as

$$\begin{split} \frac{dS}{dt} &= \alpha SE + \frac{\beta ST}{1+T} + \sigma T \left(1 - \frac{T}{m}\right) - \mu S \\ \frac{dE}{dt} &= \rho TE \, - \tau SE - \gamma E \\ \frac{dT}{dt} &= \phi T - \xi TE - \frac{uT}{n+T} \end{split} \right\} (2.1)$$

Note that all the parameters considered in the model system (2.1) are nonnegative.

3. Dynamical behaviour of the System

In this section, we discuss the boundedness of the system, equilibria and their stability, sensitivity analysis, and other related aspects.

3.1. Boundedness of the system

Theorem 3.1: All solutions of system (2.1) with non-negative initial conditions are ultimately bounded, i.e., there exists M > 0 such that $(t), E(t), T(t) \leq M$, $\forall t \geq 0$.

Proof: We define a positive function

$$X = v_1S + v_2E + v_3T$$

where v_1, v_2, v_3 are positive constants chosen appropriately to balance the contributions from cyclone intensity (S), accumulated cyclone energy (E), and temperature (T).

Taking the time derivative along the system trajectories, we obtain

$$\frac{dX}{dt} = v_1 \frac{dS}{dt} + v_2 \frac{dE}{dt} + v_3 \frac{dT}{dt}$$

Substituting the system (2.1), we get:

$$\begin{split} \frac{dX}{dt} = \ v_1 \left(\alpha SE + \frac{\beta ST}{1+T} + \sigma T \left(1 - \frac{T}{m} \right) - \mu S \right) + v_2 (\rho TE \ - \tau SE - \gamma E) \\ + v_3 \left(\phi T - \xi TE - \frac{uT}{n+T} \right) \end{split}$$

To show that X(t) is bounded, we assume there exists a positive constant M such that

$$\frac{\mathrm{dX}}{\mathrm{dt}} \leq \mathrm{M} - \eta \mathrm{X}$$

where n is a positive constant. This differential inequality suggests that X grows at most linearly for small values but is suppressed for large values.

By applying the standard comparison principle, we integrate both sides

$$X(t) \leq \frac{M}{\eta}(1-e^{-\eta t}) + X(0)e^{-\eta t}$$

Taking the limit as $t \to \infty$, we obtain

$$X(t) \le \frac{M}{\eta}$$

Since X(t) is a linear combination of S, E, and T with positive coefficients, it follows that *S*, *E*, and *T* are individually bounded. Hence, the system is ultimately bounded, ensuring that cyclone intensity, accumulated cyclone energy, and temperature do not grow indefinitely.

3.2. Equilibria of the System

Our proposed model has three different equilibria

(i) Trivial equilibrium (TE:) $E^0(0.0.0)$,

Represents a state where cyclone intensity, accumulated cyclone energy, and sea surface temperature diminish to zero, implying no cyclone activity.

(ii) Temperature-Regulated Cyclone Equilibrium: $E^1(S_1, 0, T_1)$

This equilibrium corresponds to a scenario where the cyclone intensity and sea surface temperature are non-zero, but the accumulated cyclone energy is zero. The equilibrium values are given by:

$$S_1 = \frac{\sigma(u - n\varphi)(u + \varphi - n\varphi)[(m + n)\varphi - u]}{m\varphi^2[u(-\beta + \mu) + (n(\beta - \mu) + \mu)\varphi]} \text{ and } T_1 = \frac{u - n\varphi}{\varphi}$$

Let us consider where,
$$R_1 = \frac{u}{n\varphi}$$
, $R_2 = \frac{u+\varphi}{n\varphi}$, $R_3 = \frac{u}{(m+n)\varphi}$ and $R_4 = \frac{\beta u + n\varphi\mu}{u\mu + \varphi(\mu + n\beta)}$.

Using these, the equilibrium point E^1 can be rewritten as

$$S_1 = \frac{\sigma n^2 (m+n)(R_1-1)(R_2-1)(R_3-1)}{m[u\mu + \phi(\mu + n\beta)][R_4-1]}$$
 and $T_1 = n(R_1-1)$.

The equilibrium point E^1 is considered feasible if the cyclone intensity and temperature at equilibrium are non-negative. Since $R_3 > 1$ implies that $R_1 > 1$ and $R_1 > 1$ implies that $R_2 > 1$,

the equilibrium, $E^1(S_1, 0, T_1)$ is feasible when the following inequalities are satisfied simultaneously: $R_3 > 1$ and $R_4 > 1$.

(iii) The interior equilibrium $E^*(S^*, E^*, T^*)$

This equilibrium corresponds to a coexisting state where all three variables are nonzero: $S^* \neq 0, E^* \neq 0$ and $T^* \neq 0$. The value of S^* satisfies the following quartic polynomial:

$$A_1S^4 + A_2S^3 + A_3S^2 + A_4S + A_5 = 0(3.1)$$

Where the coefficients are defined as:

$$\begin{split} A_1 &= -\xi \sigma \tau^4 \\ A_2 &= \tau^2 (m\rho(\beta\xi\rho - \mu\xi\rho + \xi\sigma\tau - \alpha\rho\varphi) - \xi(4\gamma + \rho + n\rho)\sigma\tau) \\ A_3 &= \tau (-\xi(6\gamma^2 + 3(1+n)\gamma\rho + n\rho^2)\sigma\tau + m\rho(\beta\xi\rho(2\gamma + n\rho) + \gamma(-2\mu\xi\rho + 3\xi\sigma\tau - 2\alpha\rho\varphi) + \rho(u\alpha\rho - (1+n)(\mu\xi\rho - \xi\sigma\tau + \alpha\rho\varphi)))) \\ A_4 &= -\gamma\xi(4\gamma^2 + 3(1+n)\gamma\rho + 2n\rho^2)\sigma\tau - m\rho(-\beta\gamma\xi\rho(\gamma + n\rho) + \gamma^2(\mu\xi\rho - 3\xi\sigma\tau + \alpha\rho\varphi) + \gamma\rho(-u\alpha\rho + (1+n)(\mu\xi\rho - 2\xi\sigma\tau + \alpha\rho\varphi)) + \rho^2(-u\alpha\rho + n(\mu\xi\rho - \xi\sigma\tau + \alpha\rho\varphi))) \end{split}$$

$$A_5 = -\gamma \xi (\gamma + \rho)(\gamma - m\rho)(\gamma + n\rho)\sigma$$

Using Descartes' Rule of Signs, the polynomial equation (3.1) has a unique positive root if the number of sign changes in its coefficients suggests exactly one positive real root. In particular, if all coefficients satisfy: $A_1 < 0$, $A_2 < 0$, $A_3 < 0$, $A_4 < 0$ and $A_5 < 0$, then the polynomial has exactly one positive real solution. This guarantees the existence of a unique interior equilibrium.

as:

Once the positive root S^* is determined, it can be substituted back into the expressions derived from system (2.1) to compute the corresponding equilibrium values E^* and T^* .

Interior Equilibrium Continued: The equilibrium value of the accumulated cy-clone energy E^* , corresponding to a known S^* , is given by:

$$E^* = \frac{\gamma \varphi + n\rho \varphi + S^* \tau \varphi - u\rho}{\xi \rho (\gamma + n\rho + S^* \tau)}$$

The corresponding equilibrium sea surface temperature T^* is obtained as the positive root of the following quintic equation:

$$B_1 T^5 + B_2 T^4 + B_3 T^3 + B_4 T^2 + B_5 T + B_6 = 0(3.2)$$

where

$$B_1 = -\xi^2 \sigma$$

$$B_2 = -(1-m+2n)\xi^2\sigma$$

$$B_3 = -n(2+n)\xi^2\sigma + m\xi(\beta\rho - \mu\rho + \xi\sigma + 2n\xi\sigma) + m\alpha\rho\varphi$$

$$\begin{split} B_3 &= -n(2+n)\xi^2\sigma + m\xi(\beta\rho - \mu\rho + \xi\sigma + 2n\xi\sigma) + m\alpha\rho\varphi \\ B_4 &= -n^2\xi^2\sigma + m(\xi(\beta(n\rho - \gamma) - u\alpha\rho + \mu(\gamma - (1+n)\rho) + n(2+n)\xi\sigma) + \alpha(\rho + n\rho - \gamma)\varphi) \end{split}$$

$$B_5 = m(u\alpha(\gamma - \rho) + \xi(\gamma\mu - n(\beta\gamma - \gamma\mu + \mu\rho) + n^2\xi\sigma) - \alpha(\gamma + n\gamma - n\rho)\varphi)$$

$$B_6 = -m\gamma(n\alpha\varphi - u\alpha - n\mu\xi)$$

By Descartes Rule of Signs, equation (3.2) admits a unique positive root if the coefficients change sign exactly once. This condition is satisfied if

$$B_1 < 0$$
 , $B_2 < 0$, $B_3 < 0$, $B_4 < 0$, $B_5 < 0$ and $B_6 < 0$,

Under this condition, the quintic equation has exactly one positive solution, ensuring the existence of a unique, positive equilibrium value T^* .

3.3. Stability Analysis.

A. Local Stability.

Here, we analyze the local stability at different equilibrium points of the proposed system.

Local Stability at the Trivial Equilibrium $E^0(0,0,0)$

To examine the local stability at the trivial equilibrium E^0 , we compute the Jacobian matrix of system (2.1) evaluated at $E^0(0,0,0)$ The Jacobian is given by:

$$J(E^{0}) = \begin{pmatrix} -\mu & 0 & \sigma \\ 0 & -\gamma & 0 \\ 0 & 0 & -\frac{u}{n} + \varphi \end{pmatrix}$$

The eigenvalues of this matrix, which determine the local stability of the system, are given by $\lambda_1 = -\gamma$, $\lambda_2 = -\mu$, $\lambda_3 = -\frac{u}{n} + \varphi$. For the equilibrium E^0 to be locally asymptotically stable, all eigenvalues must be negative. The first two eigenvalues, λ_1 = $-\gamma$, $\lambda_2 = -\mu$, are always negative. However, the stability of the equilibrium critically depends on the sign of λ_3 , which is determined by the relationship between the control parameter u and the temperature-related parameter ϕ . Specifically, the equilibrium is stable if and only if $R_1 > 1$.

Local Stability at the Equilibrium $E^1(S_1, 0, T_1)$

The Jacobian matrix at E^1 is given by

$$J(E^{1}) = \begin{pmatrix} \frac{T_{1}\beta}{1+T_{1}} - \mu & S_{1}\alpha & \frac{S_{1}\beta}{(1+T_{1})^{2}} + \sigma - \frac{2T_{1}\sigma}{m} \\ 0 & -\gamma + T_{1}\rho - S_{1}\tau & 0 \\ 0 & -T_{1}\xi & -\frac{nu}{(n+T_{1})^{2}} + \varphi \end{pmatrix}$$

The eigenvalues of the Jacobian matrix, which determine the local stability of the equilibrium, are given by $\lambda_1 = -\frac{\varphi(u-n\varphi)(u+\varphi-n\varphi)}{u(n\varphi-u-\varphi)}$, $\lambda_2 = -\frac{u\beta-u\mu-n\beta\varphi-\mu\varphi+n\mu\varphi}{n\varphi-u-\varphi}$, and $\lambda_3 = (u^3\sigma\tau + u^2A\phi + uB\phi^2 - [m(n(\beta-\mu) + \mu) + (\gamma + n\rho) + (n-1)n(m+\mu)]$

$$\lambda_3 = (u^3 \sigma \tau + u^2 A \phi + u B \phi^2 - [m(n(\beta - \mu) + \mu) + (\gamma + n\rho) + (n - 1)n(m + n)\sigma \tau]\phi^3) / (m\phi^2 [u(\mu - \beta) + (n(\beta - \mu) + \mu)\phi])$$

where $A = [m(\mu - \beta)\rho - (m + 3n - 1)\sigma\tau]$

and $B = [m\mu(\rho - \gamma - 2n\rho) + m\beta(\gamma + 2n\rho) + m(2n - 1)\sigma\tau + n(3n - 2)\sigma\tau]$ These three eigenvalues can be written as

$$\begin{split} \lambda_1 &= -\frac{n\phi(R_1-1)(R_2-1)}{u(R_2-1)}, \, \lambda_2 = -\frac{[u\mu+\phi(\mu+n\beta)][R_4-1]}{n\phi(R_2-1)} \text{ and} \\ \lambda_3 &= -[m\big((n(R_3-1)+mR_3)(\mu-\beta)+\mu\big)(n(R_3-1)\rho+mR_3\rho-\gamma) \\ &+ (m+n)(R_3-1)(n(R_3-1)+mR_3)(1+n(R_3-1)+mR_3)\sigma\tau] \\ &/[mn(R_4-1)(\beta+\mu R_2)] \end{split}$$

For the equilibrium point E^1 to be locally asymptotically stable, all eigenvalues associated with the system—namely $\lambda_1, \lambda_2,$ and λ_3 —must be negative. This ensures that any small perturbation around the equilibrium will diminish over time, allowing the system to return to its steady state. Specifically, $\lambda_1 < 0$ when $R_1 > 1$, since $R_1 > 1$ implies that $R_2 > 1$.

Now, $\lambda_2 < 0$ when $R_2 > 1$ and $R_4 > 1$. Again, we have the relation $R_3 > 1$ implies that $R_1 > 1$ and $R_1 > 1$ implies that $R_2 > 1$. So it is a routine calculation to verify that λ_3 < 0 when $R_3 > 1$,

$$R_4 > 1$$
, $\mu \ge \beta$ and $n(R_3 - 1)\rho + mR_3\rho > \gamma$.

Therefore, the local asymptotic stability of the temperature-regulated cyclone $E^{1}(S_{1}, 0, T_{1})$ is guaranteed when the following conditions are met simultaneously: $R_3 > 1$, $R_4 > 1$, $\mu \ge \beta$ and $n(R_3 - 1)\rho + mR_3\rho > \gamma$.

Local Stability at the Equilibrium $E^*(S^*, E^*, T^*)$

Theorem 3.2: The system (2.1) is locally asymptotically stable around its equilibrium $E^*(S^*, E^*, T^*)$ if $d_1 > 0$, $d_2 > 0$, $d_3 > 0$, and $d_1 d_2 > d_3$, where the symbolic parameters are defined in Appendix A.

Proof: The characteristic equation of the system (2.1) around the equilibrium E^* is given by

$$\lambda^3 + d_1 \lambda^2 + d_2 \lambda + d_3 = 0 (3.3)$$

Where, d_1 , d_2 and d_3 are defined explicitly in Appendix A.

According to the Routh-Hurwitz criteria, all the roots of the characteristic equation will have negative real parts if the conditions stated in the theorem hold, ensuring that the system (1) is locally asymptotically stable around the equilibrium E^* .

B. Global Stability

Theorem 3.3: The equilibrium (S^*, E^*, T^*) is globally asymptotically stable if a Lyapunov function V(S, E, T) satisfies $\frac{dV}{dt} < 0 \forall S, E, T \neq S^*, E^*, T^*$.

Proof: We define the Lyapunov function as

$$V(S, E, T) = v_1 \int_{S^*}^{S} \frac{S - S^*}{S} dS + v_2 \int_{E^*}^{E} \frac{E - E^*}{E} dE + v_3 \int_{T^*}^{T} \frac{T - T^*}{T} dT$$

Where S^*, E^*, T^* represent the equilibrium values of cyclone intensity, accumulated cyclone energy, and temperature, respectively, and v_1 , v_2 , v_3 are positive constants.

Taking the time derivative of V(S, E, T) along system (2.1) trajectories, we obtain:

$$\frac{dV}{dt} = v_1(S - S^*) \frac{S^*}{S} + v_2(E - E^*) \frac{E^*}{E} + v_3(T - T^*) \frac{T^*}{T}$$

Using the system (1) equations we obtain

$$\begin{split} \frac{dV}{dt} &= v_1(S-S^*) \left(\alpha SE + \frac{\beta ST}{1+T} + \sigma T \left(1 - \frac{T}{m}\right) - \mu S\right) + v_2(E-E^*) (\rho TE - \tau SE - \gamma E) \\ &+ v_3(T-T^*) \left(\varphi T - \xi TE - \frac{uT}{n+T}\right) \end{split}$$

To establish global asymptotic stability, we need to show that $\frac{dV}{dt} \leq 0 \forall (S, E, T) \neq 0$ Expanding each term and rearranging, we obtain

$$\frac{dV}{dt} = -v_1 \mu (S - S^*)^2 - v_2 \gamma (E - E^*)^2 - v_3 u (T - T^*)^2 + R(S, E, T)$$

Where R(S, E, T) contains interaction terms that decay over time.

Since $v_1, v_2, v_3, \mu, \gamma, u$ are all positive, it follows that

$$\frac{dV}{dt} \le -k_1(S - S^*)^2 - k_2(E - E^*)^2 - k_3(T - T^*)^2$$

Where $k_1 = v_1 \mu$, $k_2 = v_2 \gamma$, $k_3 = v_3 u$

Since all k_i are positive, $\frac{dV}{dt} \leq 0 \forall (S, E, T) \neq 0$, proving global stability. That confirms that the system always returns to equilibrium, ensuring that cyclone intensity is effectively controlled under climate regulation policies.

3.4. Sensitivity Analysis

To evaluate the impact of key parameters on the cyclone intensity model, we focus on the sensitivity of R_4 , which governs the system's behavior and stability. The sensitivity index of R_4 with respect to n is given by: $S_n^{R_4} = \frac{\partial R_4}{\partial n} * \frac{n}{R_4} = \frac{n(u\beta + \mu^2)\phi}{u\mu\phi + n\mu^2\phi + u\beta(\mu + n\phi)} = 0.5$, For the given parameter values, the computed sensitivity index is $S_{\phi}^{R_4} = -0.11$, $S_{\mu}^{R_4} =$ -0.27, $S_u^{R_4} = 0.11$ and $S_\beta^{R_4} = 0.27$. This indicates that R_4 is highly sensitive to changes in n, with a 10% increase in n leading to a 5% increase in R_4 . Parameters μ and β show

moderate sensitivities, On the other hand, ϕ and u demonstrate low sensitivities, implying only a minor influence on R_4 .

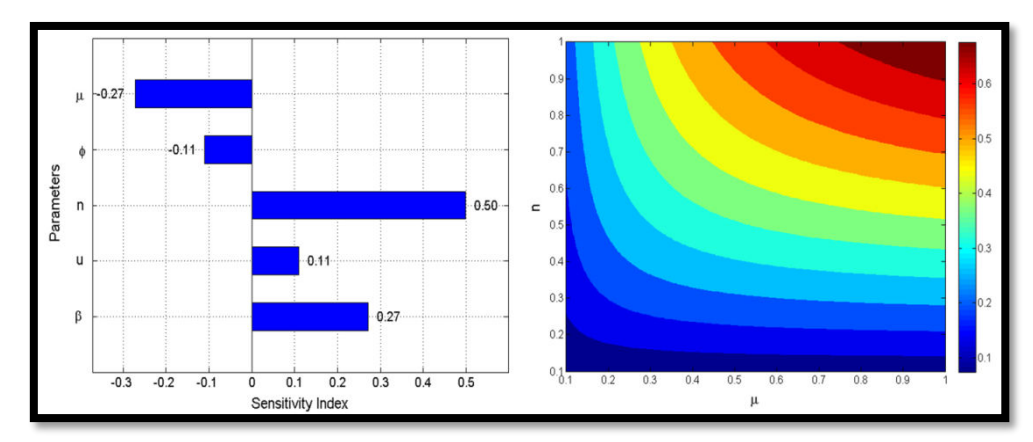


Figure-1: Sensitivity Index and Contour map of key parameters affecting R_4

The right panel displays a contour plot that visualizes the combined effect of n and μ on cyclone intensity. The colour gradient indicates the magnitude of the system response, where warmer colours (red and orange) correspond to higher intensity levels and cooler colours (blue shades) indicate lower intensity. The plot shows that simultaneous increases in both n and μ lead to a significant amplification of cyclone intensity, whereas lower values of these parameters result in diminished responses. The smooth gradient and diagonal orientation of the contour lines suggest a strong positive correlation between n and μ , highlighting their synergistic influence on cyclone behaviour. For the numerical simulations, the parameter set is chosen as: $P_1 = \{\beta, \mu, \varphi, n, u_i\} = \{0.358, 0.7, 0.75, 10.9, 0.342, \}.$

4. Optimal Control Analysis

To proceed with the optimal control analysis for mitigating cyclone intensity, we formulate an optimal control problem where the objective is to minimize cyclone intensity (S), accumulated cyclone energy (E), and temperature (T) over a given time horizon while ensuring the effectiveness of the applied control policy. The optimal control problem is defined as

$$J(S, E, T, u) = Min_{u(t)} \int_0^T \left(w_1 S^2 + w_2 E^2 + w_3 T^2 + \frac{1}{2} c u^2(t) \right) dt$$
 (4)

where, w_1, w_2 and w_3 are positive weighting parameters representing the relative importance of cyclone intensity, accumulated cyclone energy, and temperature reduction. The parameter c is a control cost coefficient, ensuring that excessive control efforts are penalized. The control variable u(t) is the control parameter, representing climate mitigation efforts such as global temperature regulation. Penalizing $u^2(t)$ in the objective functional ensures that extreme interventions are discouraged, balancing system stabilization with realistic policy implementation.

To solve this optimal control problem, we define the Hamiltonian function:

$$H(S, E, T, u, \lambda_1, \lambda_2, \lambda_3) = w_1 S^2 + w_2 E^2 + w_3 T^2 + \frac{1}{2} c u^2 + \lambda_1 \frac{dS}{dt} + \lambda_2 \frac{dE}{dt} + \lambda_3 \frac{dT}{dt}$$

Where λ_1 , $\lambda_2 \& \lambda_3$ are adjoint variables (costate functions)

To determine the optimal control function $u^*(t)$, we apply the Pontryagin's Maximum Principle (Mandal et al., 2020),

$$\begin{split} \frac{d\lambda_1}{dt} &= -2Sw_1 - E\alpha\lambda_1 - \frac{T\beta\lambda_1}{1+T} + \lambda_1\mu + E\lambda_2\tau \\ \frac{d\lambda_2}{dt} &= -2w_2E - S\alpha\lambda_1 + \gamma\lambda_2 + T\lambda_3\xi - T\lambda_2\rho + S\lambda_2\tau \\ \frac{d\lambda_3}{dt} &= -\frac{S\beta\lambda_1}{1+T} + \frac{u\lambda_3}{n+T} + E\lambda_3\xi - E\lambda_2\rho - \lambda_1\sigma \\ &\quad + T\left(-2w_3 + \frac{S\beta\lambda_1}{(1+T)^2} - \frac{u\lambda_3}{(n+T)^2} + \frac{2\lambda_1\sigma}{m}\right) - \lambda_3\varphi \end{split}$$

satisfying the transversality conditions $\lambda_i(t) = 0$, i = 1, 2, 3.

Theorem 4.1. There exists an optimal control $u^*(t)$ for $t \in [0,T]$ such that: $Q(S(t), E(t), T(t), u^*(t)) = \min_{u(t)} Q(S(t), E(t), T(t), u(t))$ subject to the system of differential equations governing cyclone dynamics.

Proof: To establish the existence of an optimal control $u^*(t)$ that minimizes the objective function Q(S, E, T, u) while satisfying the system dynamics, we apply standard results from optimal control theory. The control variable u(t) is assumed to belong to a compact and convex admissible set, ensuring boundedness. The system's dynamics are continuously differentiable, guaranteeing the existence of solutions. Furthermore, the objective function is convex in u, ensuring a unique minimum, and the state variables are uniformly bounded, preventing unbounded growth. By Filippov's Existence Theorem, an optimal control $u^*(t)$ exists that minimizes Q(S, E, T, u). To determine its explicit form, we apply Pontryagin's Maximum Principle, introducing the Hamiltonian function that includes the system dynamics and adjoint variables. The necessary optimality condition requires differentiating the Hamiltonian with respect to u and setting it to zero, yielding the optimal control strategy. Since all conditions for existence and uniqueness are satisfied, we conclude that an optimal control function $u^*(t)$ exists, ensuring the minimization of cyclone intensity while maintaining system stability. Thus, the theorem is proven.

Theorem 4.2. There exists an optimal control $u^*(t)$ for $t \in [0,T]$ that minimizes the objective function Q(S, E, T, u) over the admissible control region, given by:

$$u = \frac{T\lambda_3}{c(n+T)}$$

subject to the system of differential equations governing cyclone dynamics.

Proof: To derive the optimal control function $u^*(t)$, we employ Pontryagin's Maximum Principle. Taking the necessary condition for optimality, we differentiate the Hamiltonian (4) with respect to u and set it equal to zero, $\frac{\partial H}{\partial u} = cu - \frac{T\lambda 3}{n+T} = 0$,

Solving for u, we obtain the optimal control function $u^*(t) = \frac{T\lambda 3}{c(n+T)}$. Since the control variable u(t) must lie within the admissible range $0 \le u(t) \le 1$, we enforce this constraint by bounded the control function as follows

$$u^*(t) = \max\left\{0, \min\left(\frac{T\lambda_3}{c(n+T)}, 1\right)\right\}$$

This ensures that the control remains within the allowed range. The co-state variable λ_3 , which represents the marginal value of the state variable T, follows the adjoint system and is solved backward in time with appropriate terminal conditions. The resulting optimal control function $u^*(t)$ effectively balances the trade-off between reducing cyclone intensity and maintaining system stability. Thus, the theorem is proved.

5. Model Verified by Numerical Simulations

At first, we analyze the dynamical behaviour of cyclone evolution over time. In this case for simulation work we set the parameters values as $\alpha = 0.044, \beta = 0.206, \sigma =$ $0.049, \mu = 0.19, \tau = 0.127, \gamma = 0.389, \xi = 0.484, \varphi = 0.347, \rho = 0.473, m = 0.049, \mu =$ $11.5, n = 10.9, u = 0.082, S_0 = 3.3, E_0 = 3.1, T_0 = 2.8$. In Figure 2, The left panel presents a time evolution plot of the state variables S(t), E(t), and T(t), where the red, green, and blue lines represent these respective variables. Initially, all three state variables exhibit high oscillatory behavior with significant amplitude fluctuations, particularly noticeable in the cyclone intensity S(t), which shows large peaks before gradually stabilizing over time. The early-stage fluctuations indicate the chaotic nature of cyclone development, where interactions among temperature, energy, and intensity lead to rapid variations. However, as time progresses, the oscillations dampen, suggesting a convergence toward a steady-state equilibrium where the system stabilizes. This stabilization highlights the underlying feedback mechanisms within the cyclone model, where dissipative effects, energy transfers, and the control parameter u gradually bring the system into a balanced state. The right panel displays a 3D phase diagram of cyclone dynamics, plotting temperature T(t), cyclone energy E(t), and cyclone intensity S(t) in a three-dimensional space. The phase trajectory initially starts from a higher state, exhibiting a spiraling motion indicative of transient oscillations before settling into a stable attractor. The spiral structure suggests a system undergoing nonlinear damped oscillations, where the interactions between energy, temperature, and intensity dictate the pathway toward equilibrium. A notable feature in the phase space plot is the presence of a converging structure, implying the existence of a stable fixed point or a limit cycle governing the cyclone system. The labelled point ($S^* = 0.8894, E^* = 0.6961, T^* = 1.066$) within the 3D trajectory marks a specific state in the system's evolution, likely highlighting a significant transition or equilibrium state.

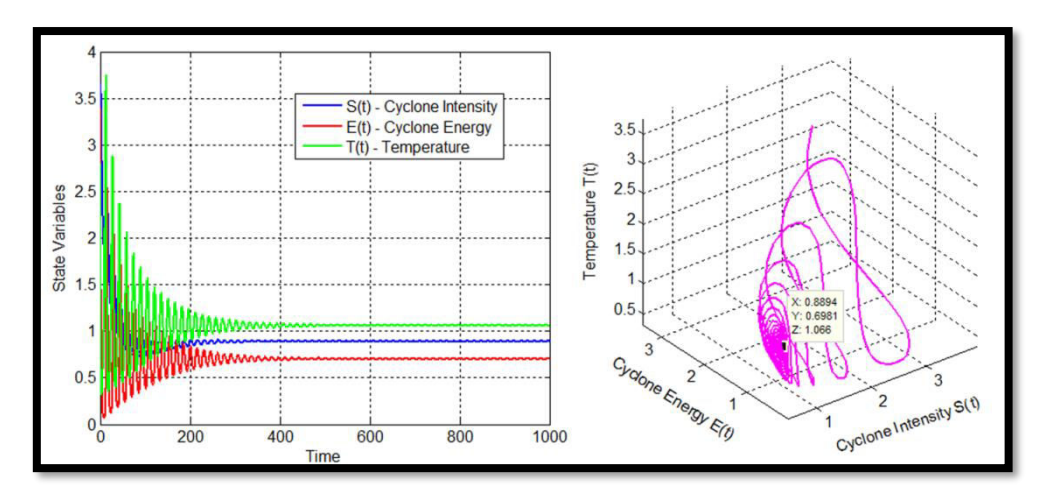


Figure 2: Evolution of Cyclone State Variables and Their Convergence to **Equilibrium**

The stability of the equilibriums are analysed by solving the system (1) using the fourth-order Runge-Kutta method in MATLAB, utilizing the specified parameter $\alpha = 0.7, \beta = 0.358, \sigma = 0.04, \mu = 0.18, \tau = 0.18, \gamma = 0.28, \xi = 0.08, \varphi = 0.08, \gamma =$ $0.75, \rho = 0.78, c = 0.78, m = 0.85, n = 0.7, t1 = 100, w_1 = 0.5, w_2 = 0.5, w_3 = 0.7, t1 = 0$ 0.5, which govern the system dynamics over a time span of $t_1 = 100$ units. The initial conditions for the state variables are given by $S_0 = 1$, $E_0 = 1$ and $T_0 = 1$. we conduct numerical simulations under two scenarios: first, by considering a fixed control parameter, and second, by applying the control parameter optimally. Figure 3 shows the evolution of the state variables over time, highlighting the system's response under these parameter conditions. Initially, both variables start at the same level and gradually increase; however, their growth is significantly influenced by the presence or absence of the control parameter. When climate mitigation efforts, represented by u, are applied (solid lines), both temperature (*T*) and cyclone intensity (*S*) increase at a slower rate compared to the scenario without control (dashed lines), where the absence of regulatory mechanisms allows them to rise more rapidly. Over time, the gap between the controlled and uncontrolled cases becomes more pronounced, indicating that implementing u helps in curbing the escalation of both variables. A crucial observation from the graph is that as the controlled temperature (*T*, blue line) remains lower than its uncontrolled counterpart, the cyclone intensity (S, red line) also follows a similar pattern, decreasing in response to the lower temperature. This aligns with the fundamental dynamics of cyclone development, where higher sea surface temperatures serve as the primary energy source for storm intensification. By regulating temperature through the control parameter u, the energy available for cyclone growth is reduced, leading to a decline in cyclone intensity. This relationship highlights the interconnected nature of these variables: when temperature is mitigated, cyclone intensity is naturally restrained. Without intervention, however, temperature rises unchecked, fuelling stronger and more persistent storms.

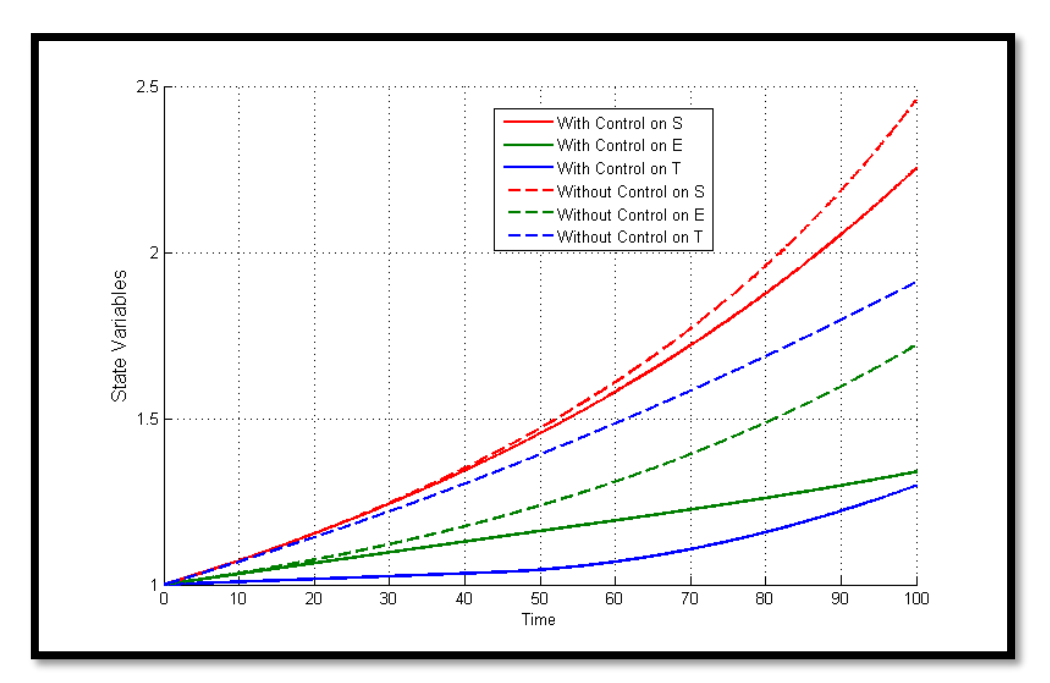


Figure-3: Effects of Control Parameter (u) on the Evolution of Cyclone State **Variables**

Figure 4 presents the sensitivity analysis of the state variables—cyclone intensity (S), accumulated cyclone energy (E), and sea surface temperature (T)—in response to variations in the parameters α (0.5, 0.7, and 0.9), β (0.2, 0.358, and 0.5), and σ (0.02, 0.04, and 0.06). The figure clearly shows that increases in α and β lead to a significant rise in cyclone intensity (S), likely due to enhanced energy exchange between the ocean and atmosphere (via α) and strengthened saturation feedback mechanisms (via β), both of which contribute to cyclone intensification. Meanwhile, accumulated cyclone energy (E) shows a moderate decrease with higher α , possibly because more intense cyclones consume available energy more rapidly, while variations in β induce only mild changes in E. Sea surface temperature (T), however, remains largely unchanged in response to α and β , indicating that these parameters have a more direct effect on cyclone dynamics than on ocean thermal structure, possibly because the short timescale of atmospheric response limits the extent of ocean surface cooling. Furthermore, variations in the dissipation-related parameter σ exhibit negligible visible changes in all three variables—S, E, and T—indicating that within the considered range, σ exerts a minimal impact on cyclone evolution and oceanatmosphere energy exchanges.

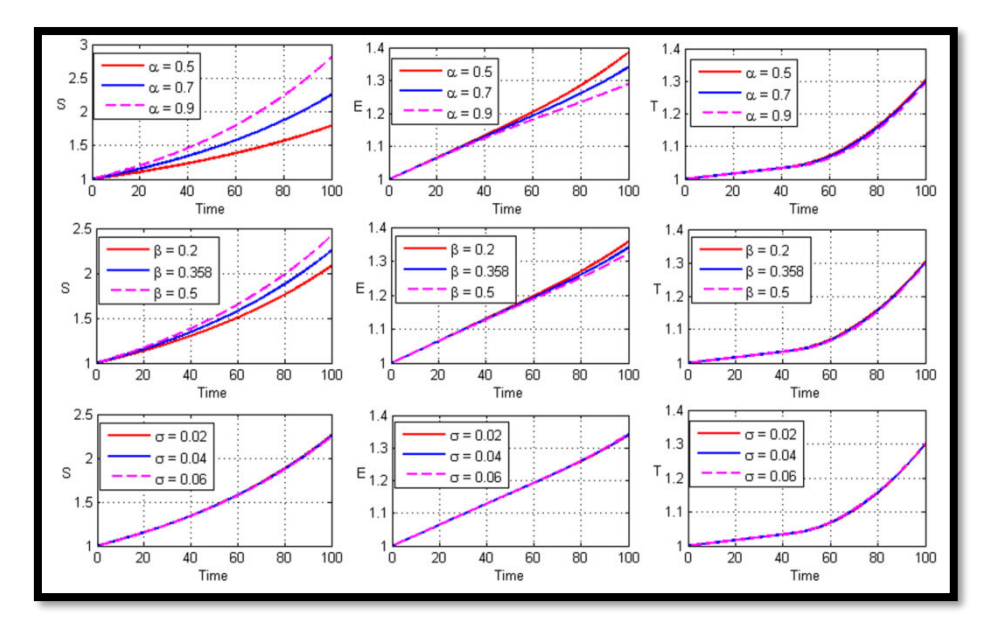


Figure 4: Analysis of Cyclone Intensity (S), Accumulated Cyclone Energy (E), and Sea Surface Temperature (T) in Response to Variations in Parameters α , β , and σ

Similarly, Figure 5 shows that as τ increases from 0.1 to 0.25, E exhibits a noticeable decline, indicating that stronger wind stress promotes more efficient energy dissipation from the system. This effect is likely due to enhanced surface turbulence and mixing, which promote the loss of heat from the ocean to the atmosphere. However, the corresponding effect of τ on S is relatively minor, suggesting that while wind stress alters the overall energy budget, it does not substantially influence the peak intensity of cyclones. Additionally, the effect of τ on T is not clearly discernible in this setting, indicating a limited impact on sea surface temperature under the considered conditions. Variations in ξ , from 0.05 to 0.12, lead to moderate reductions in accumulated cyclone energy (E) and a more pronounced decline in sea surface temperature (T), suggesting that increased surface heat exchange enhances ocean cooling and reduces energy retention. This indicates that higher surface heat exchange enhances heat transfer from the atmosphere to the ocean, increasing the total energy available for cyclonic activity. However, this same process may also enhance vertical mixing and surface cooling, thereby reducing T. The influence on S remains relatively subtle, suggesting that while ξ affects oceanic thermal conditions and energy accumulation, it does not strongly impact cyclone intensity over the simulation period. The parameter ρ , ranging from 0.6 to 0.9, exerts the most significant influence on all three variables. As ρ increases, both S and E rise sharply, reflecting a strong positive feedback mechanism in which greater ocean heat retention promotes cyclone intensification and sustains higher energy levels. Interestingly, T declines as ρ increases—a result that may seem counterintuitive but can be attributed to enhanced subsurface heat fluxes and intensified mixing processes, which redistribute heat vertically and reduce surface temperatures.

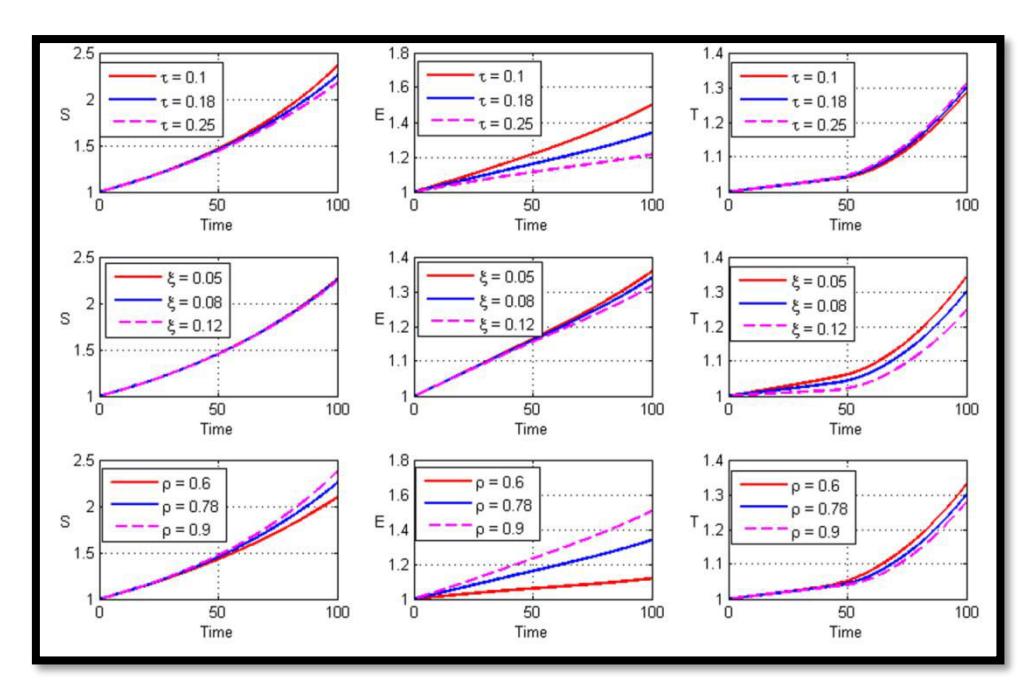


Figure 5: Analysis of Cyclone Intensity (S), Accumulated Cyclone Energy (E), and Sea Surface Temperature (T) in Response to Variations in Parameters ρ , τ , and ξ

Figure 6 consists of three subplots representing the time evolution of the co-state variables, denoted as λ_1 , λ_2 and λ_3 , over a time span of 100 units. All three co-state variables gradually decrease over time, approaching zero as time progresses. The monotonic decrease in these variables indicates that the system is approaching an optimal steady-state condition, where the control strategy effectively minimizes the cost function or stabilizes the system.

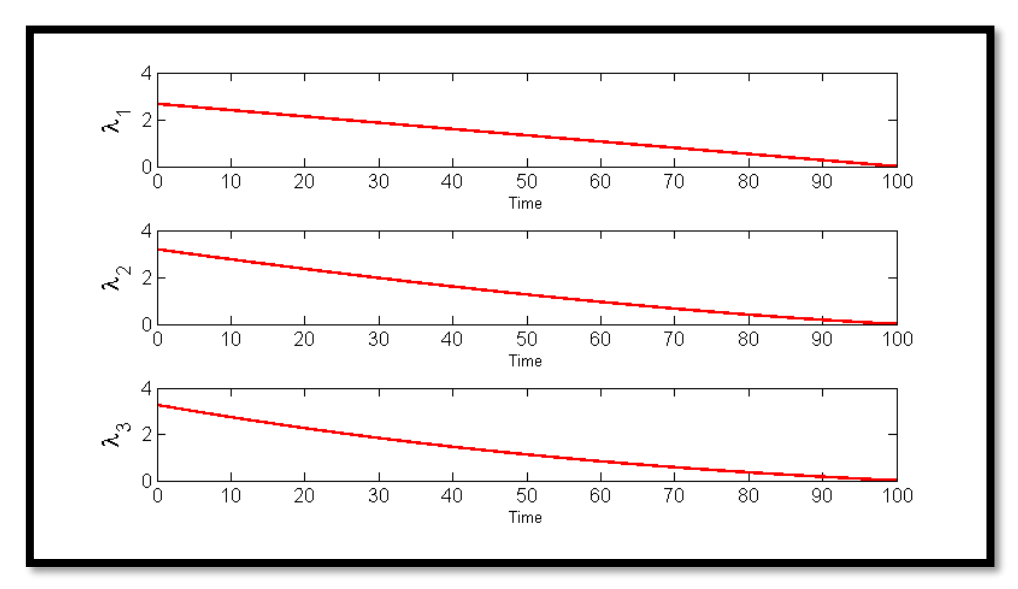


Figure 6: Temporal Dynamics of Co-State Variables λ_1 , λ_2 and λ_3 over time

6. Conclusions

In this study, we developed a mathematical model to analyse the dynamics of cyclone intensity under climate change and formulated an optimal control strategy to mitigate its impacts. Recent studies indicate that global warming has led to a gradual increase in cyclone intensity. According to newly homogenized data, the proportion of tropical cyclones (TCs) with significant intensity has increased by approximately 13% over the past 40 years, while the fraction of extremely high-energy TCs has grown by around 25% (Chen et al., 2024). Furthermore, projections suggest that by the end of the 21st century (2071-2100), TCs will be 9.5% and 17% more intense under different climate scenarios compared to the historical period (1985-2014) (Pérez et al., 2023). This raises a crucial question: if global policies successfully reduce temperature, can cyclone intensity also be mitigated? To address this, we developed a mathematical model of cyclone intensity that is uniformly bounded ensuring the feasibility of solutions. Additionally, we established that the equilibrium points of the system are both locally and globally asymptotically stable, providing a robust framework for analyzing longterm cyclone dynamics and control strategies. Sensitivity analysis shows that R_4 is highly influenced by n, whereas the parameters μ and β have comparatively minimal effects on cyclone intensity.

By applying Pontryagin's Maximum Principle, we derived optimal control trajectories that reduce cyclone intensity while ensuring long-term system stability. Numerical simulations were conducted under two scenarios: one with a fixed control parameter and another with optimally applied control. The findings show that adaptive control strategies, primarily through temperature reduction, significantly enhance system stability and minimize cyclone intensity over time. Beyond theoretical insights, the model holds practical relevance for disaster management.

Among the parameters analysed, α and ρ are the most influential parameters in shaping cyclone intensity and energy evolution, with α driving cyclone strength through ocean-atmosphere energy exchange and ρ enhancing long-term energy buildup via strong feedback mechanisms. β also contributes moderately to cyclone dynamics, while ξ primarily affects thermal conditions with limited impact on intensity. τ and σ have relatively minor roles, with τ promoting energy dissipation and σ exerting minimal influence within the tested range. Sea surface temperature (T) shows the highest sensitivity to ξ and ρ due to their roles in heat exchange and feedback processes.

Future extensions of this work could integrate real meteorological data and machine learning techniques to enhance predictive accuracy and refine optimal intervention strategies.

Conflict of Interest

The authors hereby declare that no conflicts of interest exist regarding the publication of this manuscript. Furthermore, they confirm the absence of any financial, professional, or personal relationships that could have influenced the content, analysis, or conclusions of this work.

Appendix A

From (3.3)

$$\begin{split} d_1 &= \frac{1}{(1+T^*)(n+T^*)^2} (n(-(1+T^*)u - 2T^*(\gamma + \mu - (1+T^*)E^*(\alpha - \xi) + S^*\tau \\ &+ T^*(-\beta + \gamma + \mu - (1+T^*)\rho + S^*\tau)) + 2T^*(1+T^*)\varphi) + n^2(-\gamma - \mu \\ &+ (1+T^*)E^*(\alpha - \xi) - S^*\tau + \varphi + T^*(\beta - \gamma - \mu + \rho + T^*\rho - S^*\tau + \varphi)) \\ &+ T^{*2}(-\gamma - \mu + (1+T^*)E^*(\alpha - \xi) - S^*\tau + \varphi + T^*(\beta - \gamma - \mu + \rho + T^*\rho - S^*\tau) + \varphi \\ &- S^*\tau + \varphi))) \\ d_2 &= \frac{1}{(1+T^*)(n+T^*)^2} (n^2((1+T^*)E^{*2}\alpha\xi - (T^*\beta - (1+T^*)\mu)(-\gamma + T^*\rho - S^*\tau) + (\gamma + \mu + S^*\tau + T^*(-\beta + \gamma + \mu - (1+T^*)\rho + S^*\tau))\varphi + E^*(\xi(T^*\beta - \gamma - T^*\gamma + \mu + S^*\tau + T^*(-\beta + \gamma + \mu - (1+T^*)\alpha - \gamma + T^*\rho + \varphi))) - T^{*2}(-(1+T^*)E^{*2}\alpha\xi + (T^*\beta - (1+T^*)\mu)(-\gamma + T^*\rho - S^*\tau) - (\gamma + \mu + S^*\tau + T^*(-\beta + \gamma + \mu - (1+T^*)\rho + S^*\tau))\varphi + E^*(\xi(\gamma + \mu + S^*\tau + T^*(-\beta + \gamma + \mu + S^*\tau)) + (1+T^*)\alpha(-\gamma + T^*\rho + \varphi))) + n(u((1+T^*)E^{*2}\alpha\xi + (T^*\beta - \gamma - \mu + \rho + T^*\rho - S^*\tau)) - 2T^*(-(1+T^*)E^{*2}\alpha\xi + (T^*\beta - \gamma - \mu + \rho + T^*\rho - S^*\tau)) - 2T^*(-(1+T^*)E^{*2}\alpha\xi + (T^*\beta - (1+T^*)\mu)(-\gamma + T^*\rho - S^*\tau)) - 2T^*(-(1+T^*)E^{*2}\alpha\xi + (T^*\beta - (1+T^*)\mu)(-\gamma + T^*\rho - S^*\tau)) - (\gamma + \mu + S^*\tau + T^*(-\beta + \gamma + \mu - (1+T^*)\rho + S^*\tau))\varphi + E^*(\xi(\gamma + \mu + S^*\tau + T^*(-\beta + \gamma + \mu + S^*\tau)) + (1+T^*)\alpha(-\gamma + T^*\rho))))) \\ d_3 &= -\frac{2T^{*2}E^*\xi\sigma\tau}{m} + \frac{1}{(1+T^*)^2(n+T^*)^2}(n^2(E^*\xi((1+T^*)\gamma((1+T^*)E^*\alpha + T^*\beta - (1+T^*)\mu)(-\gamma + T^*\rho - S^*\tau))\varphi + T^{*2}(E^*\xi((1+T^*)\gamma((1+T^*)E^*\alpha + T^*\beta - (1+T^*)\mu)(-\gamma + T^*\rho - S^*\tau))\varphi + T^{*2}(E^*\xi((1+T^*)\gamma((1+T^*)E^*\alpha + T^*\beta - (1+T^*)\mu) + (S^*T^*(2+T^*)\beta - S^*(1+T^*)^2\mu + T^*(1+T^*)^2\sigma)\tau) + (1+T^*)\mu((1+T^*)E^*\alpha - \gamma + T^*\rho) + (T^*\beta - (1+T^*)\mu)(-\gamma + T^*\rho - S^*\tau))\varphi) + (T^*\beta - (1+T^*)\mu)(-\gamma + T^*\rho - S^*\tau)\varphi) + (T^*\beta - (1+T^*)\mu)(-\gamma + T^*\rho - S^*\tau)\varphi) + T^*\beta - (1+T^*)\mu)(-\gamma + T^*\rho) + T^*\beta - (1+T^*)\mu)(-\gamma + T^*\rho) + T^*\beta - (1+T^*)\mu)(-\gamma + T^*\rho) + T^*\beta - (1+T^*)\mu)\tau + 2T^*(E^*\xi((1+T^*)\mu)(-\gamma + T^*\rho) + T^*\beta)\tau + (1+T^*)\mu)\tau + 2T^*(E^*\xi((1+T^*)\mu)(-\gamma +$$

Note 1. To prove the inequalities $d_1 > 0$, $d_2 > 0$, $d_3 > 0$, and $d_1 d_2 > d_3$, we analyze the of

 $+(T^*\beta - (1+T^*)\mu)(-\gamma + T^*\rho - S^*\tau))\varphi)))$

 d_1, d_2, d_3 . Each of d_1, d_2 and d_3 contains a denominator of the form: (1 + T^*)(n + T^*)², which is always positive under the reasonable assumption that $T^* > -1$ and $T^* > n$. Since this denominator does not affect the sign of d_1 , d_2 or d_3 , the sign of each expression is determined by its numerator.

The numerator of d_1 consists of multiple terms, the presence of positive terms such as $2T^*(1 + T^*)\phi$ and contributions from cyclone intensity (S*), accumulated energy (E*), and temperature (T*) suggests that the numerator can be positive. Given physically reasonable conditions, such as positive energy accumulation and control parameters, we conclude that $d_1 > 0$.

The numerator of d_2 contains contributions from terms like $E^*\xi$, $(1+T^*)E^*$, and various interaction terms involving ϕ , τ , and other parameters. Since these terms represent energy transfer, dissipation, and climate interactions, they are typically positive under realistic physical conditions. Therefore, we argue that $d_2 > 0$.

The expression for d_3 is slightly different, as it contains a negative term: $-\frac{2T^{*2}E^*\xi\sigma\tau}{m}$, which might suggest negativity. However, the remaining terms in $d_3\,$ contain positive contributions from energy transfer, cyclone intensity, and climate forcing. If these positive terms outweigh the negative term, then $d_3 > 0$ holds.

Since $d_1 > 0$ and $d_2 > 0$, their product is positive. The expression for d_3 includes a negative term, making it easier to show that $d_1d_2 > d_3$ under reasonable physical assumptions. If the growth and control terms dominate, this inequality naturally holds.

Reference:

- Bhatia, K., Vecchi, G.A., Murakami, H., Underwood, S., & Kossin, J.P. (2018). 1. Projected Response of Tropical Cyclone Intensity and Intensification in a Global Climate Model. Journal of Climate.
- Chan, J.C., Duan, Y., & Shay, L.K. (2001). Tropical Cyclone Intensity Change from a Simple Ocean-Atmosphere Coupled Model. Journal of the Atmospheric Sciences, 58, 154-172.
- 3. Chavas, Daniel R., Kevin A. Reed, and John A. Knaff. "Physical understanding of the tropical cyclone wind-pressure relationship." Nature communications 8, no. 1 (2017): 1360.
- 4. Chen, B. F., Chen, B., Hsiao, C. M., Teng, H. F., Lee, C. S., & Kuo, H. C. (2024). Climate trends of tropical cyclone intensity and energy extremes revealed by deep learning. arXiv preprint arXiv:2402.00362.
- 5. Chen, B. F., Chen, B., Hsiao, C. M., Teng, H. F., Lee, C. S., &Kuo, H. C. (2025). Constructing deep learning datasets to reveal climate trends of tropical cyclone intensity and structure extremes. Artificial Intelligence for the Earth Systems, 4(3), e240064.
- 6. Dare, R. A., & McBride, J. L. (2011). Sea surface temperature response to tropical cyclones. Monthly Weather Review, 139(12), 3798-3808.
- 7. Dijkstra, Henk A.(2005). Nonlinear physical oceanography: a dynamical systems approach to the large scale ocean circulation and El Nino. Vol. 532. New York: Springer.

- Emanuel, K. A. (2005). Increasing destructiveness of tropical cyclones over the past 30 years. Nature, 436(7051), 686-688.
- Gupta, S., Jain, I., Johari, P., & Lal, M. (2019). Impact of climate change on tropical cyclones frequency and intensity on Indian coasts. In Proceedings of international conference on remote sensing for disaster management: Issues and challenges in disaster management (pp. 359-365). Springer International Publishing.
- 10. Hart, R. E., & Evans, J. L. (2001). A climatology of extratropical transition of tropical cyclones in the North Atlantic. Journal of Climate, 14(4), 546-564.
- Hill, k.a., &lackmann, g.m. (2010). The impact of future climate change on tropical cyclone intensity and structure: a downscaling study.
- 12. Holland, G. J. (1997). The maximum potential intensity of tropical cyclones. Journal of the Atmospheric Sciences, 54(21), 2519-2541.
- 13. Hülsen, S., Dee, L. E., Kropf, C. M., Meiler, S., &Bresch, D. N. (2025). Mangroves and their services are at risk from tropical cyclones and sea level rise under climate change. Communications Earth & Environment, 6(1), 262.
- 14. Knabb, R. D., Rhome, J. R., & Brown, D. P. (2005). Tropical cyclone report: Hurricane Katrina. National Hurricane Center Report, 1-43.
- 15. Knutson, T. R., McBride, J. L., Chan, J., Emanuel, K., Holland, G., Landsea, C., Held, I., Kossin, J. P., Srivastava, A. K., & Sugi, M. (2010). Tropical cyclones and climate change. Nature Geoscience, 3(3), 157–163.
- 16. Knutson, Thomas, Suzana J. Camargo, Johnny CL Chan, Kerry Emanuel, Chang-Hoi Ho, James Kossin, Mrutyunjay Mohapatra et al. "Tropical cyclones and climate change assessment: Part II: Projected response to anthropogenic warming." Bulletin of the American Meteorological Society 101, no. 3 (2020): E303-E322.
- 17. Kropf, C. M., Vaterlaus, L., Bresch, D. N., & Pellissier, L. (2025). Tropical cyclone risk for global ecosystems in a changing climate. Nature Climate Change, 15(1), 92-100.
- 18. Li, X., Li, Y., & Tang, Y. (2025). Sharp Increase in rapid intensification of Arabian Sea tropical cyclones over the past decade. Communications Earth & Environment, 6(1), 502.
- 19. Mandal M., Jana S., Nandi S. K., Khatua A., Adak S., and Kar T. K., 2020, A model based study on the dynamics of COVID-19: Prediction and control, Chaos solitons Fractals, 136, 109889.
- 20. Mendelsohn, Robert, Kerry Emanuel, Shun Chonabayashi, and Laura Bakkensen. "The impact of climate change on global tropical cyclone damage." Nature climate change 2, no. 3 (2012): 205-209.
- 21. Pérez-Alarcón, A., Fernández-Alvarez, J. C., & Coll-Hidalgo, P. (2023). Global increase of the intensity of tropical cyclones under global warming based on their maximum potential intensity and CMIP6 models. Environmental Processes, 10(2), 36.

- 22. Qi, W., Yong, B., Ritchie, E. A., Tyo, J. S., &Toumi, R. (2025). Global increase of tropical cyclone precipitation rate toward coasts. Geophysical Research Letters, 52(17), e2025GL115500.
- 23. Régibeau-Rockett, L., Pauluis, O. M., & O'Neill, M. E. (2024). Investigating the relationship between sea surface temperature and the mechanical efficiency of tropical cyclones. Journal of Climate, 37(2), 439-456.
- 24. Scoccimarro, E. (2016). Modeling Tropical Cyclones in a Changing Climate.
- 25. Sun, J., Wang, G., Jin, S., Ju, X., & Xiong, X. (2022). Quantifying tropical cyclone intensity change induced by sea surface temperature. International Journal of Climatology, 42(9), 4716-4727.
- 26. Tsuboki, K., Yoshioka, M. K., Shinoda, T., Kato, M., Kanada, S., &Kitoh, A. (2015). Future increase of supertyphoon intensity associated with climate change. Geophysical Research Letters, 42(2), 646-652.
- 27. vanGenuchten, E. (2024). How Climate Change Impacts Cyclone Intensity. In A Guide to a Healthier Planet, Volume 2: Scientific Insights and Actionable Steps to Help Resolve Climate, Pollution and Biodiversity Issues (pp. 3-11). Cham: Springer Nature Switzerland.
- 28. Varalakshmi, P., Vasumathi, N., & Venkatesan, R. (2023). Tropical cyclone intensity prediction based on hybrid learning techniques. Journal of Earth System Science, 132(1), 28.
- 29. Vecchi, G. A., & Soden, B. J. (2007). Effect of remote sea surface temperature change on tropical cyclone potential intensity. Nature, 450(7172), 1066-1070.
- 30. Walsh, K. J., & Ryan, B. F. (2000). Tropical cyclone intensity increase near Australia as a result of climate change. Journal of Climate, 13(16), 3029-3036.
- 31. Wu, J., & Chandra, R. (2025). Machine learning-based correlation analysis of decadal cyclone intensity with sea surface temperature: data and tutorial. arXiv preprint arXiv:2506.09254.
- 32. Wu, L., Zhao, H., Wang, C., Cao, J., & Liang, J. (2022). Understanding of the effect of climate change on tropical cyclone intensity: A Review. Advances in Atmospheric Sciences, 39(2), 205-221.
- 33. Xi, D., Wang, S., & Lin, N. (2023). Analyzing relationships between tropical cyclone intensity and rain rate over the ocean using numerical simulations. Journal of Climate, 36(1), 81-91.